Electronic Supplementary Information

Rational synthesis and dimensionality tuning of MOFs from preorganized heterometallic molecular complexes

Aleksandr A. Sapianik,[*,a,b] Mikhail A. Kiskin,[c] Konstantin A. Kovalenko,[a,b] Denis G. Samsonenko,[a,b] Danil N. Dybtsev,[*,a,b] Nathalie Audebrand,[d] Yaguang Sun,[e] and Vladimir P. Fedin [a,b]

[a]Nikolaev Institute of Inorganic Chemistry SB RAS, 3 Akad. Lavrentiev Av., 630090 Novosibirsk, Russia

[b]N. S. Kurnakov Institute of General and Inorganic Chemistry, RAS, 31 Leninsky Av., 119991 Moscow, Russia

[c]Novosibirsk State University, 2 Pirogova st., 630090 Novosibirsk, Russia

[d]Univ Rennes, CNRS, ISCR (Institut des Sciences Chimiques de Rennes) - UMR 6226, F-35000 Rennes, France

[e]Laboratory of Coordination Chemistry, Shenyang University of Chemical Technology, Shenyang 110142, People's Republic of China.

X-ray crystallography. The fragments of the heterometallic complex **1** and coordination polymers **2**, **3**, **5dmf** and **6dma** in thermal ellipsoid mode are presented in Figures S1, S2, S4. Additional figures, highlighting the structure projections and inner surfaces of the frameworks **3** and **5dmf** are presented in Fig. S3, S5.Topological presentation of 3D and 2D nets of obtained compounds are shown on Figure S6.

Powder X-ray diffraction analyses. The PXRD data for the as synthesized, host-guest compounds and for samples after sorption experiments on Figures S7-12. There are additional lines at 12° on Figures S11, S12. The origin of which is due to different solvent content between calculated and measure data (SQUEEZE procedure was carried out for **6dmf** data).

Le Bail fit. Calculated unit cell parameters and pattern-matching for compounds 4 are provided on Figures S13-15.

Thermogravimetric analyses. The TGA plots for the reported compounds are presented in Figure S16.

FT-IR spectroscopy. The IR spectra of the compounds are present in Figure S17.

Gas (N_2, CO_2, CH_4) adsorption isotherm measurements and IAST calculations. The analyses were performed on Quantochrome's Autosorb iQ at 77 K (nitrogen) and 195 K (carbon dioxide) and 298K (CO_2, CH_4). The gas adsorption/desorption isotherms for the activated **4dmf, 5dmf, 5dma** and **6dmf** are provided on Figures S18-S20. Capacities of CO_2, CH_4 loads are presented in Table S1. Heats of adsorption is presented in Table S2. Henry constants and selectivities are presented in Tables S3-S5. IAST calculation predictions at different temperatures are presented in Figures S21, S22.

Benzene/cyclohexane separation. ^{1}H-NMR spectra of **6dmf** exposed to a solution of a benzene/cyclohexane mixture (1:1) for 24 hours is presented in Figure S23.

Luminescent properties. Spectra of emission (λ_{ex} = 300 nm) and excitation of **4dmf·G** (G = nitrobenzene, 2,6-dimethylnitrobenzene and 4-nitro-*m*-xylene) and as synthesized compound **4dmf** are shown on Figure S24.

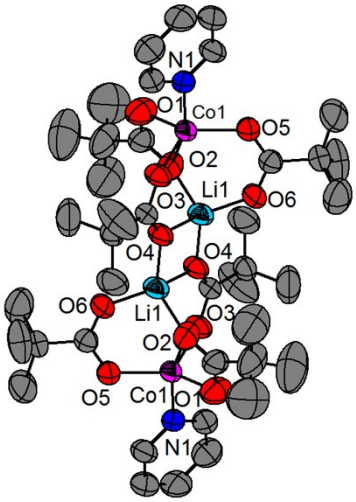

Figure S1. $[Li_2Co_2(piv)_6(py)_2]$ ellipsoid model representation (hydrogen atoms are omitted; ellipsoids are at the 50% probability level).

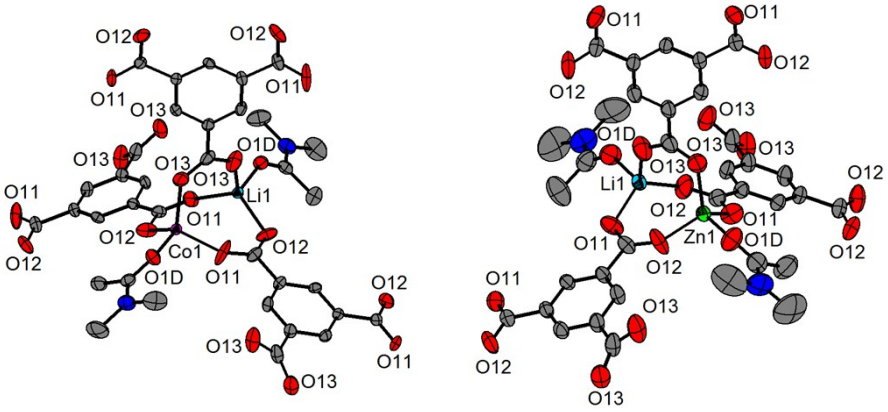

Figure S2. Ellipsoid model representation in **2** and **3** (hydrogen atoms are omitted; ellipsoids are at the 50% probability level; Li cations are presented as blue balls, Co – as pink, Zn – as green).

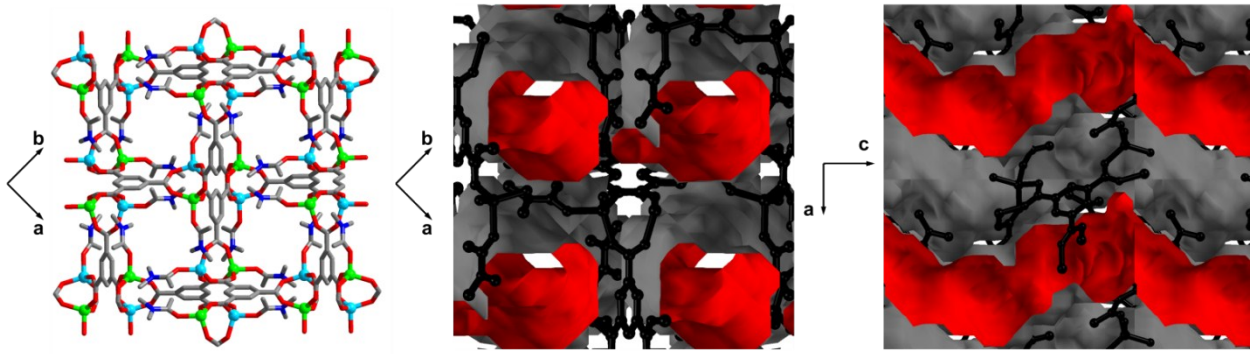

Figure S3. Structure projection of **3** with channel views (Li cations are presented as blue balls, Zn – as green). Calculated inner void surface id shown as red.

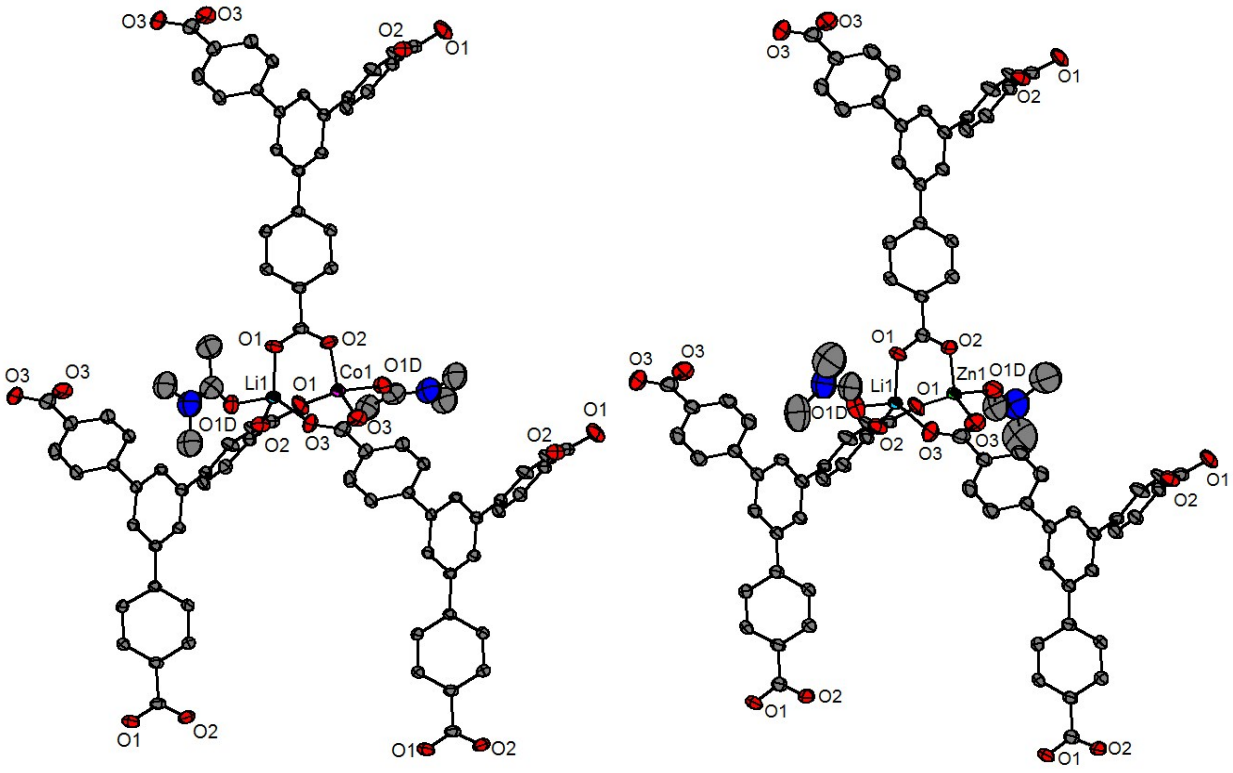

Figure S4. Ellipsoid model representation in **5dma** and **6dmf** (hydrogen atoms are omitted; ellipsoids are at the 50% probability level; Li cations are presented as blue balls, Co – as pink, Zn – as green).

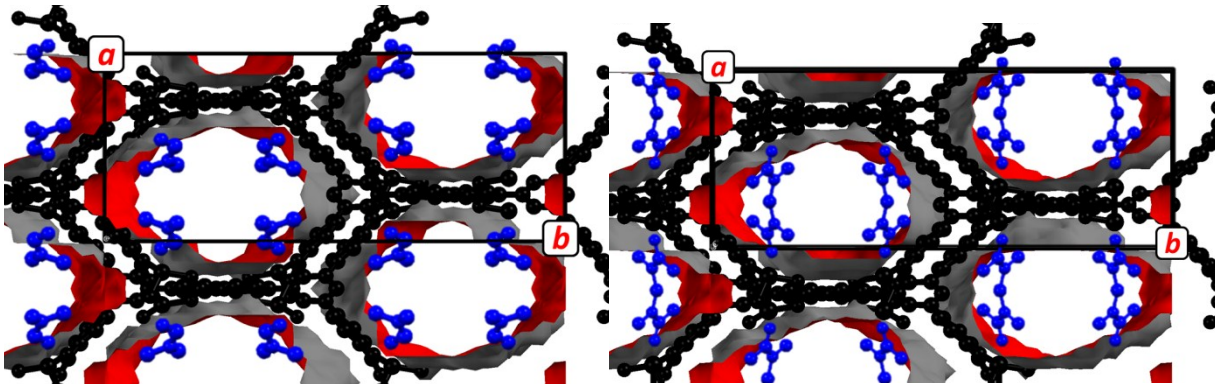

Figure S5. Projection of structure **6dmf** (left) and **5dma** (right) on the *ab* plane with calculated void surfaces.

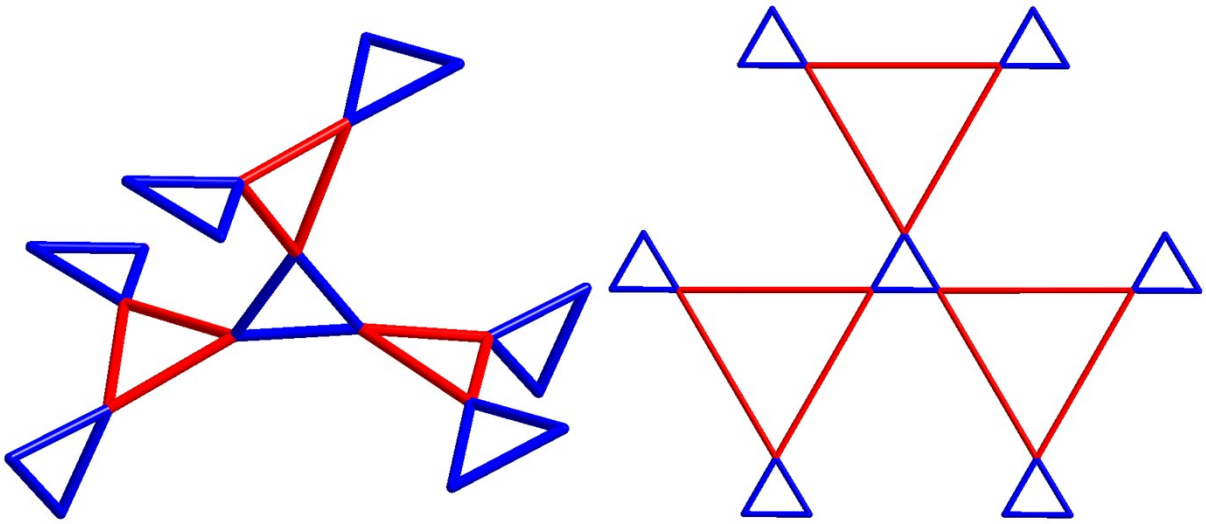

Figure S6. Topological representation of structure of **2** (left) and **5**, **6** (right). {LiM$(COO)_3$}units are shown as blue triangles, tricarboxylate ligands – as red triangles.

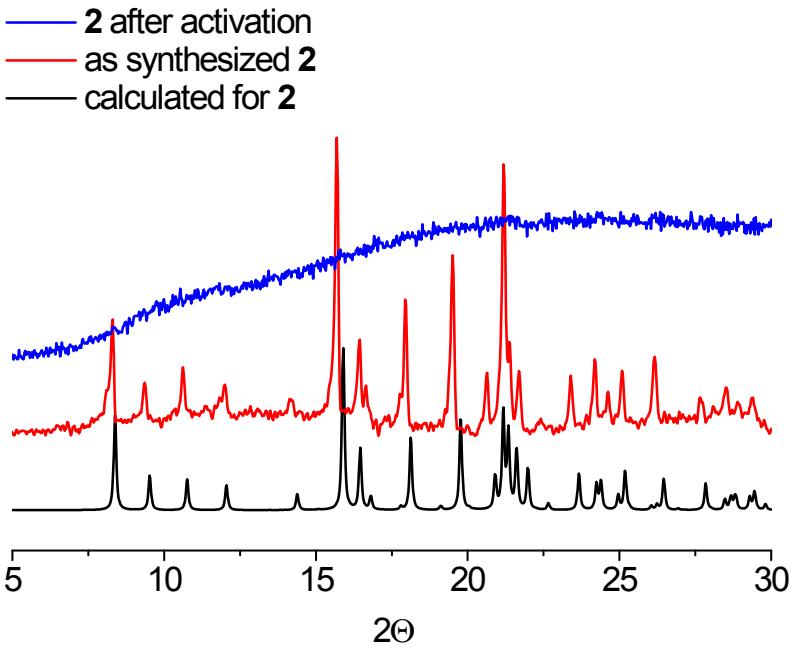

Figure S7. PXRD pattern for **2** as synthesized, after activation and calculated from SXRD experiment.

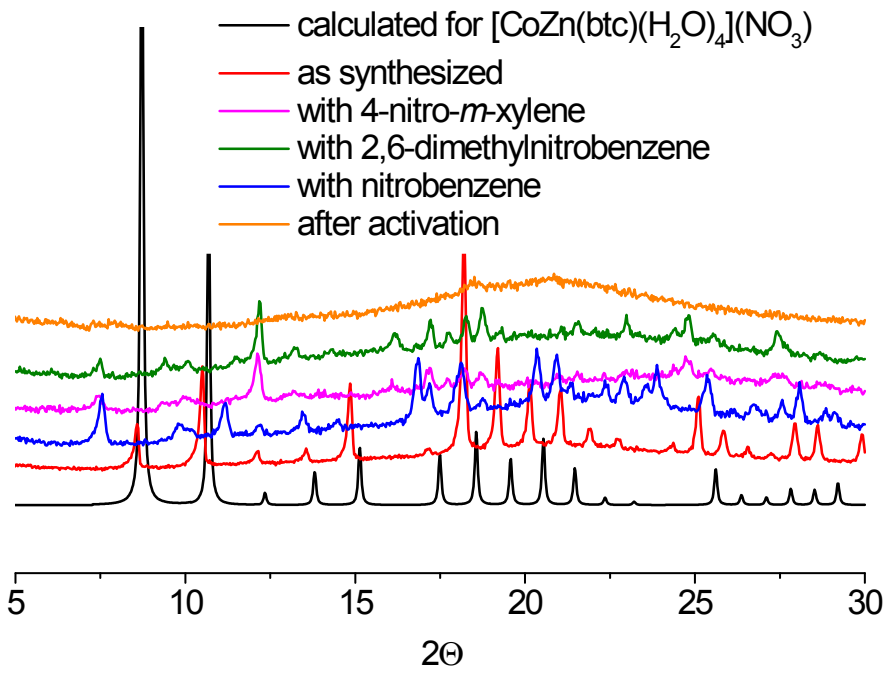

Figure S8. PXRD pattern for as synthesized **4dmf**, **4dmf·G** and after activation.

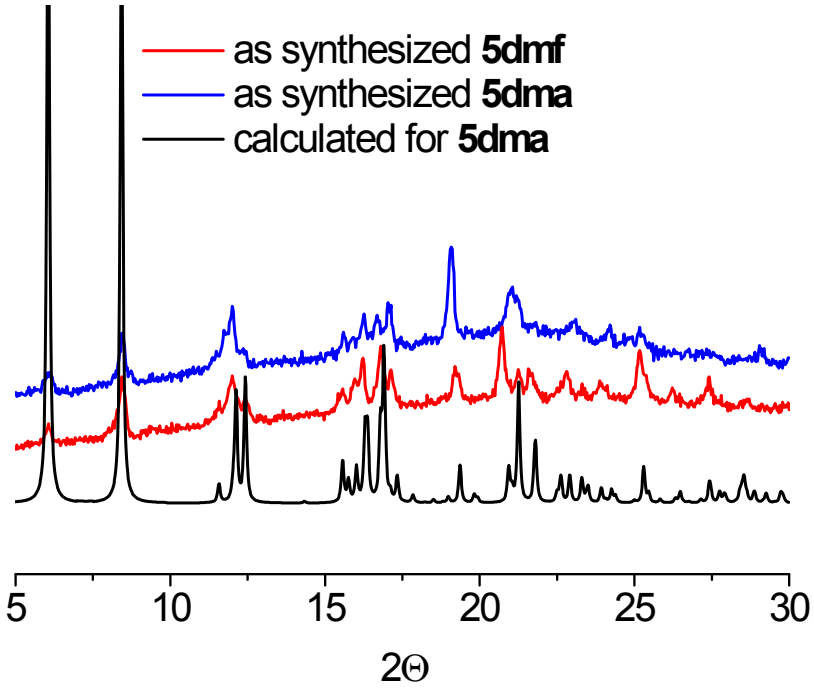

Figure S9. PXRD pattern for **5dmf** and **5dma** as synthesized and calculated from SXRD experiment for **5dma**.

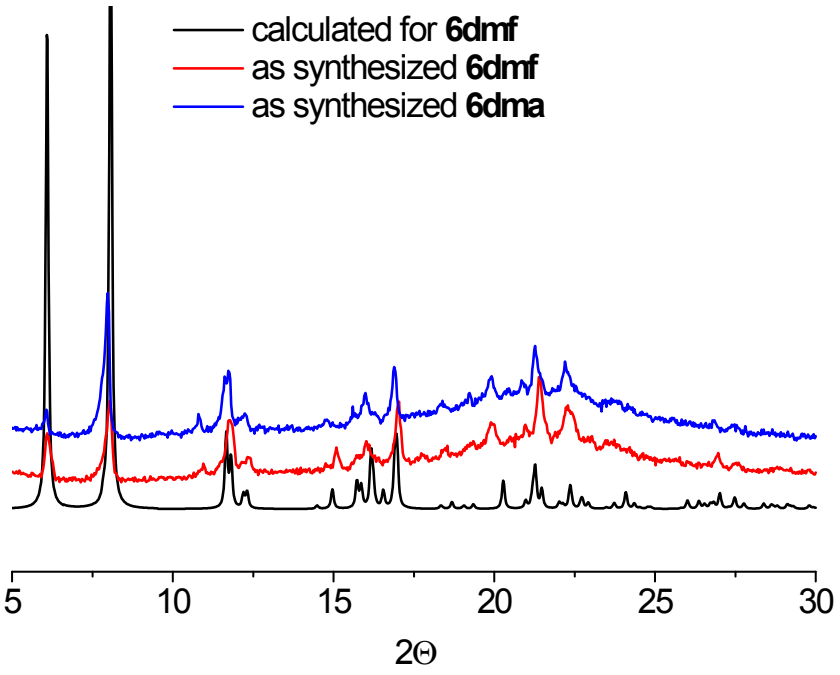

Figure S10. PXRD pattern for **6dmf** and **6dma** as synthesized and calculated from SXRD experiment for **6dmf**.

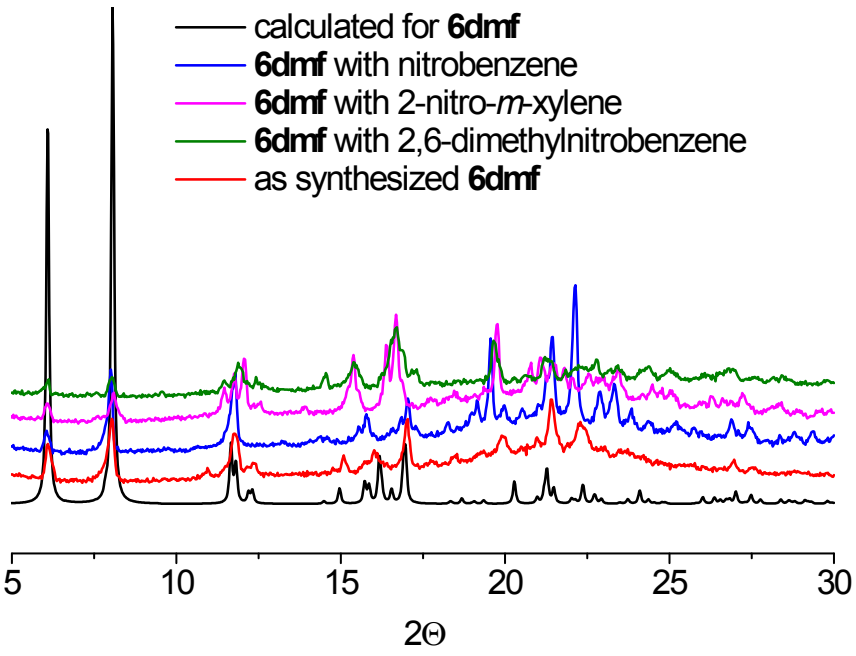

Figure S11. PXRD pattern for **6dmf·G**.

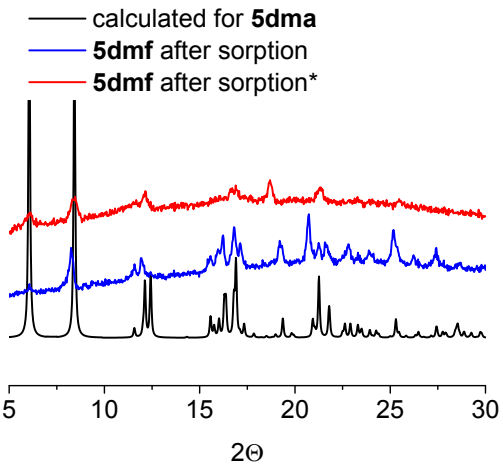

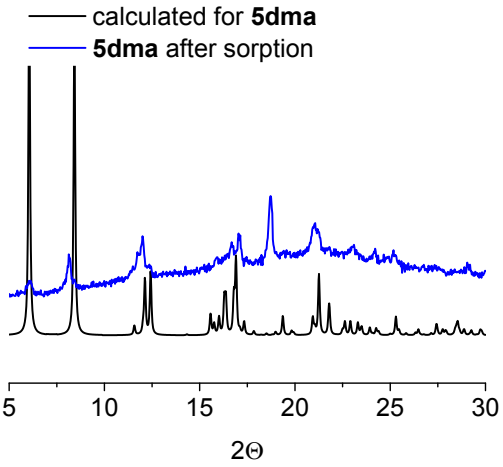

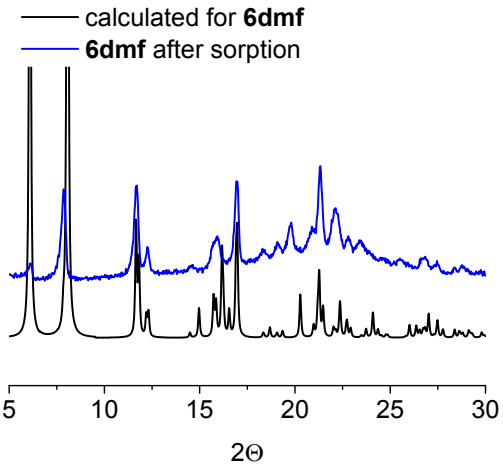

Figure S12. PXRD pattern for **5dmf, 5dma** and **6dmf** after gas sorption experiments in comparison with calculated from SXRD experiment for **5dma** and **6dmf**. * – sample was additionally vacuumated at 120°C for 4 hours

4dmf

- Cubic cell: 14.356(2) / $P2_13$
=> Rp: 3.53 Rwp: 4.63 Rexp: 3.00 Chi2: 2.37

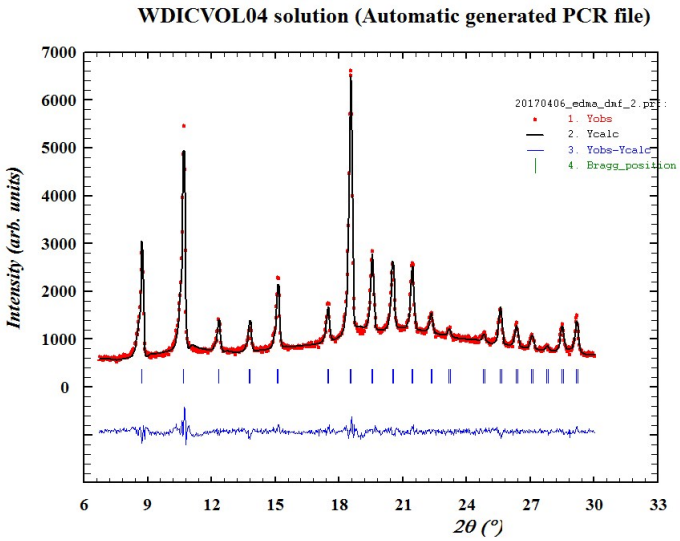

Figure S13. Pattern-matching for **4dmf**

4dma

- Cubic unit-cell : a = 14.338(3) / $P2_13$
=> Rp: 3.30 Rwp: 4.25 Rexp: 3.17 Chi2: 1.80

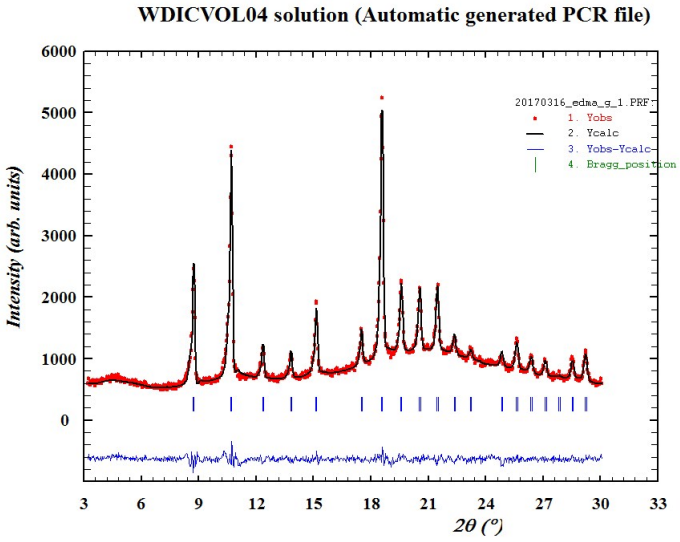

Figure S14. Pattern-matching for **4dma**

4nmp

- Cubic cell: 14.494(4) / $P2_13$
=> Rp: 7.20 Rwp: 11.0 Rexp: 4.15 Chi2: 6.99

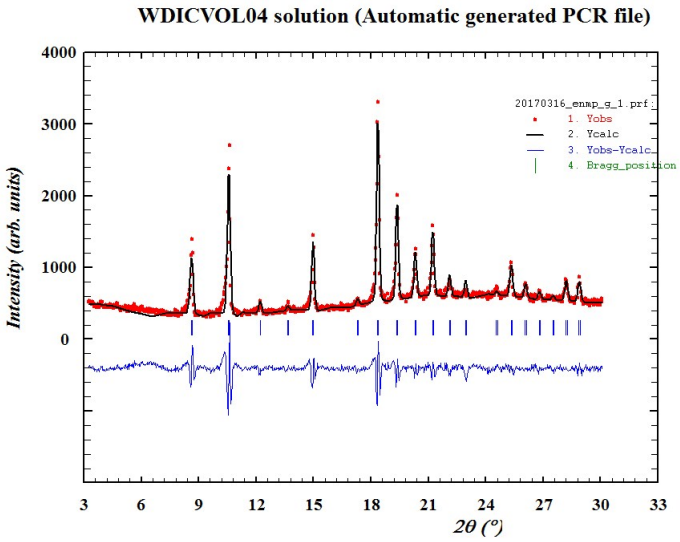

Figure S15. Pattern-matching for **4nmp**

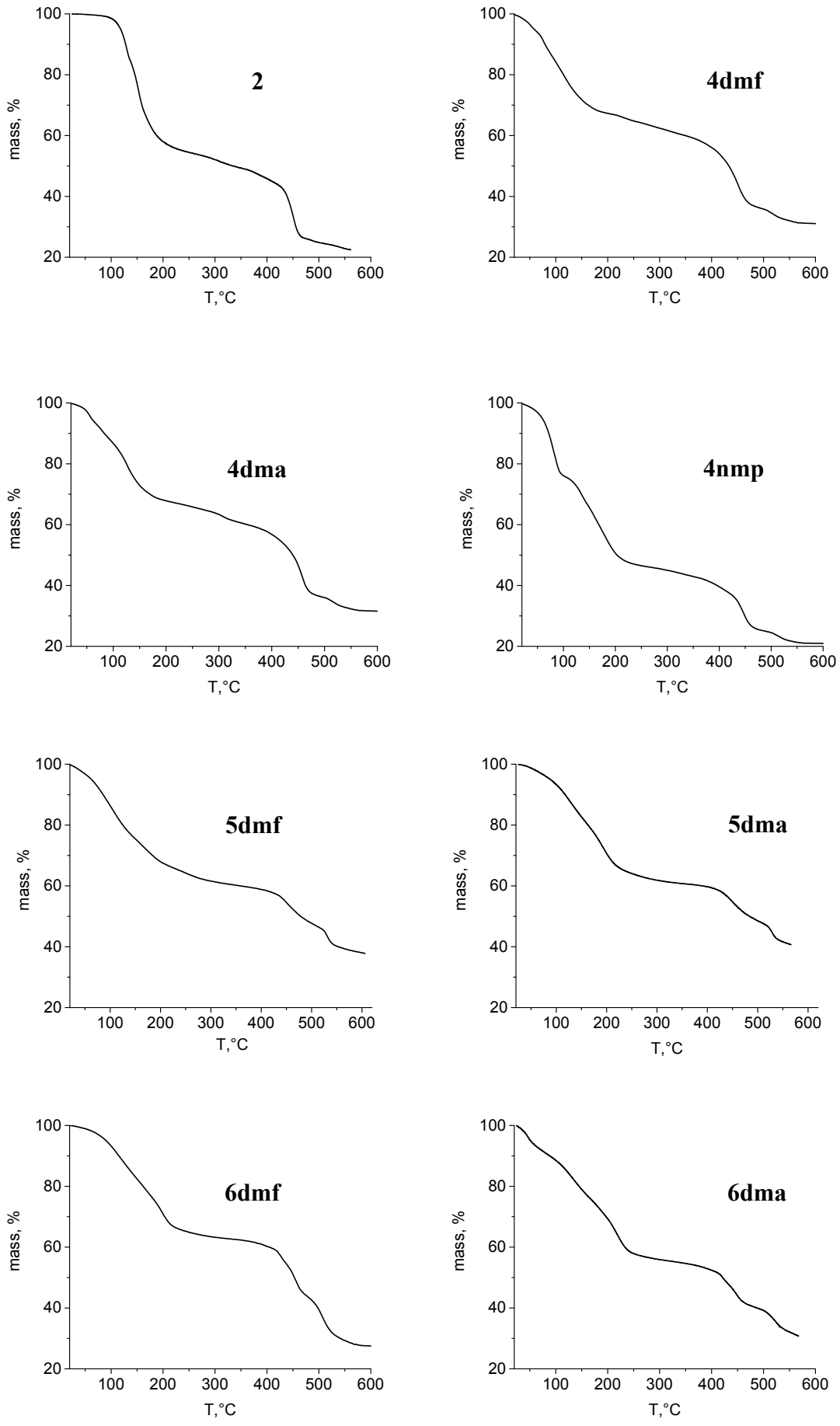

Figure S16. TGA plots for **2–6**.

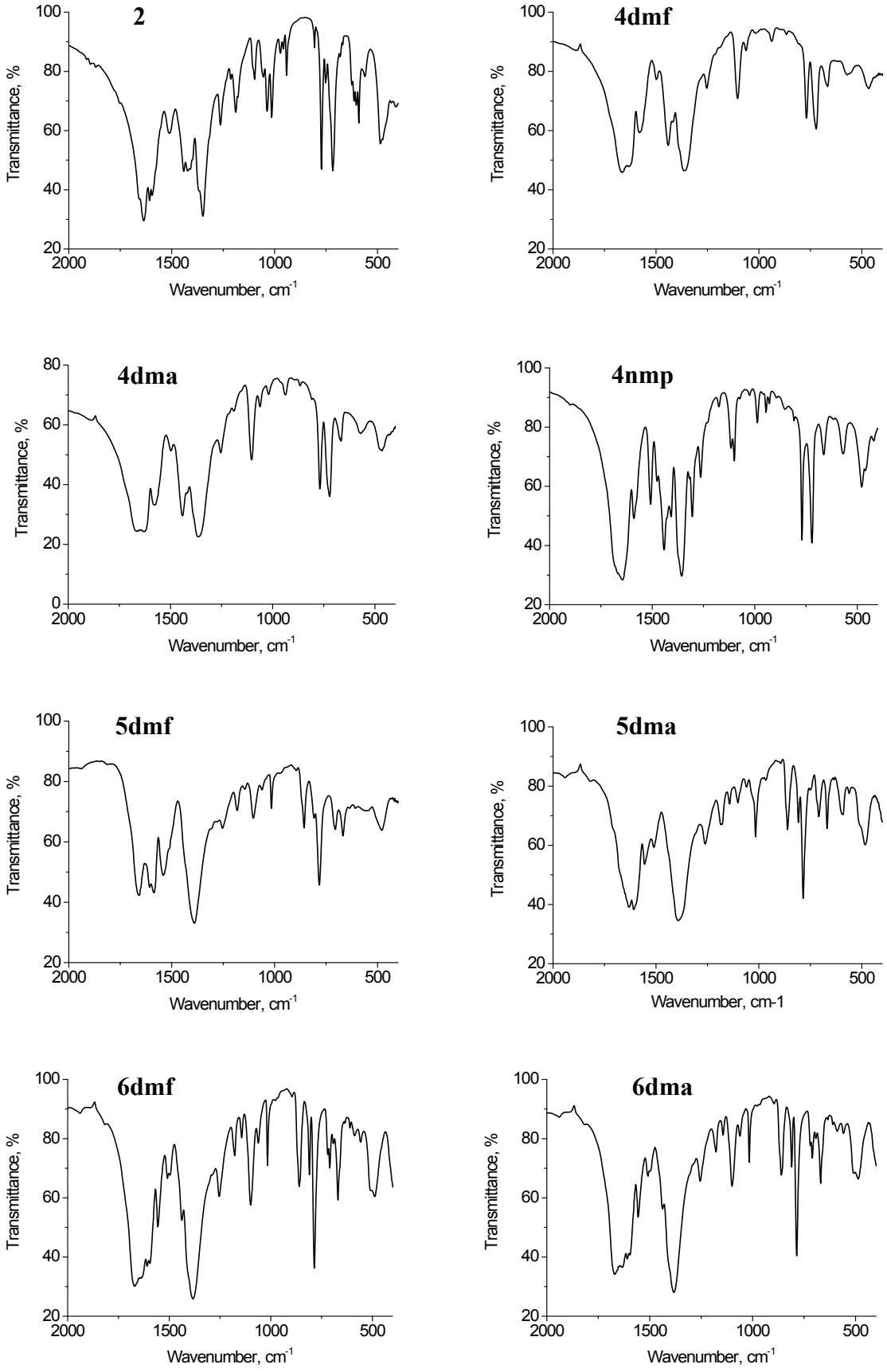

Figure S17. FT-IR spectra of **2–6**.

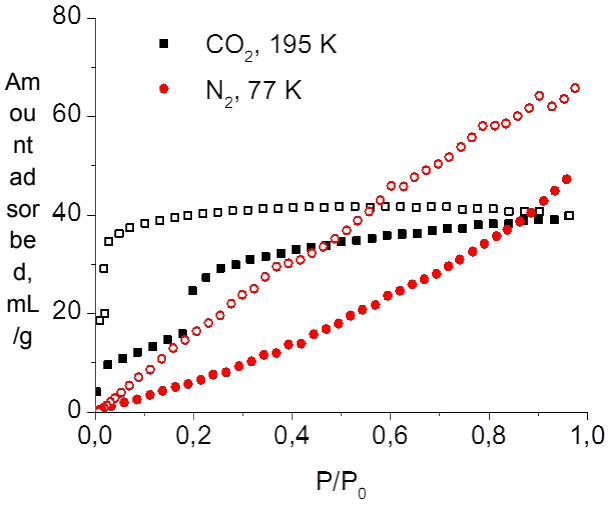

Figure S18. N_2 (77 K) and CO_2 (195 K) sorption isotherms for activated **4dmf.**

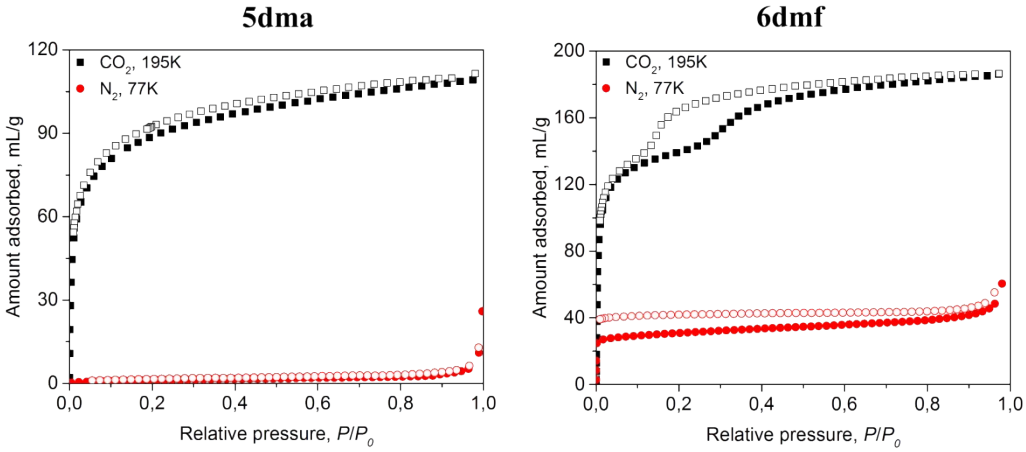

Figure S19. Adsorption−desorption isotherms of N_2 at 77K and CO_2 at 195K by **5dma** and **6dmf**.

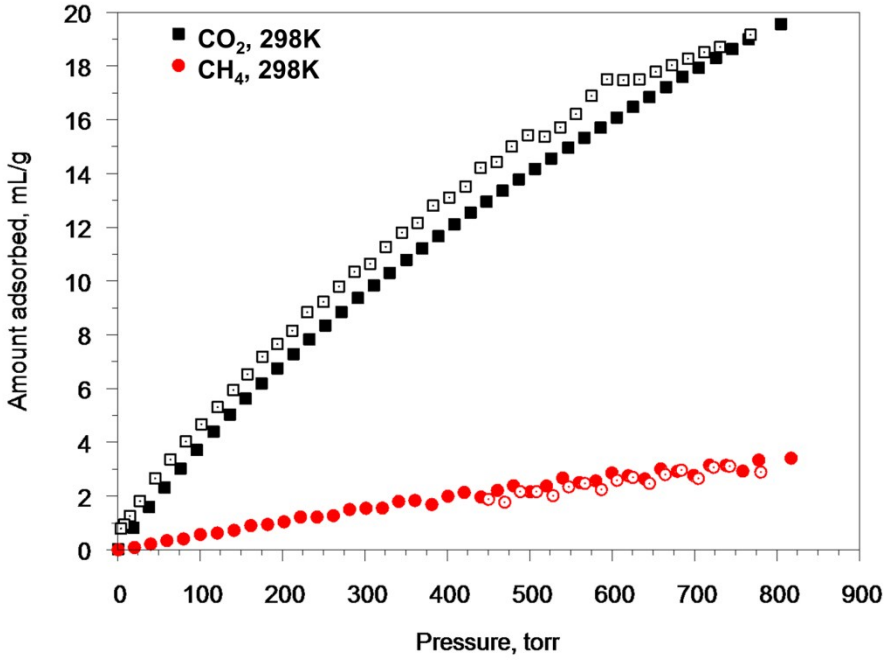

Figure S20. Adsorption isotherms of CO_2 and CH_4 at 298 K by activated **5dmf**.

Table S1**.** Carbon dioxide and nitrogen uptakes by **5dmf** at 1 bar and 273K or 298K.

Units	**CO_2**		**CH_4**		**N_2**
	273K	**298K**	**273K**	**298K**	**273K**
mL/g	29.95	18.96	7.48	2.93	2.76
mmol/g	1.34	0.846	0.333	0.131	0.123
wt. %	5.88	3.72	0.54	0.21	0.35

Heats of adsorption

Heats of adsorption were calculated by means of virial approach. To that isotherms at 273K and 298K were fitted by virial equation:

$$\ln p = \ln n + \frac{1}{T}\sum_i A_i \cdot n^i + \sum_j B_j \cdot n^j \quad (1)$$

Isosteric heats of adsorption were calculated using virial coefficients by equation (2):

$$Q_{st} = R \cdot \sum_i A_i \cdot n^i \quad (2)$$

Table S2**.** Zero-coverage heats of adsorption in kJ/mol.

Sample	**CO_2**	**CH_4**
5dmf	26.9	25.1

Henry constants

Henry constants for CO_2 and CH_4 isotherms were calculated using virial coefficients by equation (3):

$$K_h = \exp\left[\frac{-A_0}{T} - B_0\right] \tag{3}$$

N_2 adsorption isotherm at 273K were fitted by Henry equation:

$$n[\text{mL/g}] = K_h \cdot p[\text{torr}] \tag{4}$$

Table S3**.** Henry constants in mmol·g^{-1}·bar^{-1} for gas adsorption by **5dmf** at 273K or 298K.

Units	**CO_2**		**CH_4**		**N_2**
	273K	**298K**	**273K**	**298K**	**273K**
mmol·g^{-1}·bar^{-1}	3.926	1.455	0.4125	0.1630	0.1248
mL·g^{-1}·torr^{-1}					0.003727

Selectivity

Adsorption selectivity factors for CO_2/N_2 or CO_2/CH_4 binary gas mixtures were calculated using three different approaches:

1) As the molar ratio of the adsorption quantities at the relevant partial pressures of the gases:

$$S = \frac{n_1/n_2}{p_1/p_2},$$

where S is the selectivity factor, n_i represents the adsorbed amount of component i, and p_i represents the partial pressure of component i.

2) As a ratio of Henry constants which corresponds to the slope of the adsorption isotherm at very low partial pressures:

$$S = \frac{K_{H1}}{K_{H2}}$$

3) By ideal adsorbed solution theory (IAST). The relationship between P, y_i and x_i (P — the total pressure of the gas phase, y_i — mole fraction of the i-component in gas phase, x_i — mole fraction of the i-component in absorbed state) is defined according to the IAST theory [1]:

$$\int_{p=0}^{p=\frac{Py_1}{x_1}} n_1(p)\,d\ln p = \int_{p=0}^{p=\frac{Py_2}{x_2}} n_2(p)\,d\ln p$$

In this case the selectivity factors were determined as:

$$S = \frac{y_2/x_2}{y_1/x_1} = \frac{x_1(1-y_1)}{y_1(1-x_1)}$$

For IAST calculations adsorption isotherms were primary fitted by appropriate model. Models used are summarized in Table S4, and below table the mathematical equations are giving for each model as well.

Table S4**.** Adsorption isotherms models for IAST calculations.

Sample	273 K			298 K	
	CO_2	**CH_4**	**N_2**	**CO_2**	**CH_4**
5dmf	LF [a]	L [b]	H [c]	LF	L

[a] Langmuir-Freundlich equation $n[\mathrm{mL/g}]=\frac{w\,b\,p[\mathrm{torr}]^{1/t}}{1+b\,p[\mathrm{torr}]^{1/t}}$;

[b] Langmuir equation $n[\mathrm{mL/g}]=\frac{w\,b\,p[\mathrm{torr}]}{1+b\,p[\mathrm{torr}]}$;

[c] Henry equation $n[\mathrm{mL/g}]=K_H\cdot p[\mathrm{torr}]$.

Calculated selectivity factors are summarized in Table 3 and Table S5. The graphs of IAST prediction curves and dependence of selectivity factors on mole fraction of CO_2 in gas phase are shown in Figs. S18–19.

Table S5**.** Calculated adsorption selectivity factors on **5dmf** for equimolar binary gas mixtures at 298K.

Gas mixture	V_2/V_1	K_{h2}/K_{h1}	IAST
CO_2/CH_4	6.5	8.9	6.5

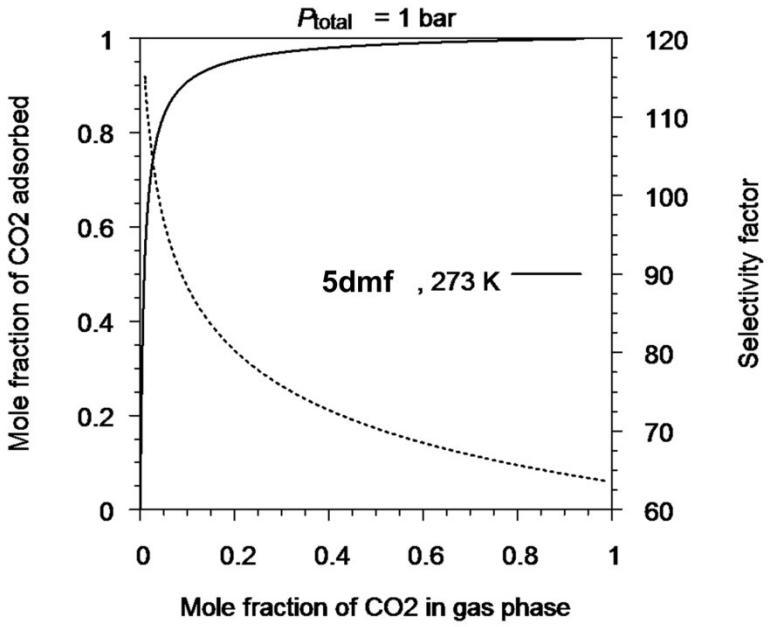

Figure S21. The adsorption equilibrium prediction by IAST for CO_2/N_2 binary mixture on **5dmf** (solid line) and the dependence of CO_2/N_2 adsorption selectivity on the CO_2 mole fraction in gas phase (dashed line) at 273K.

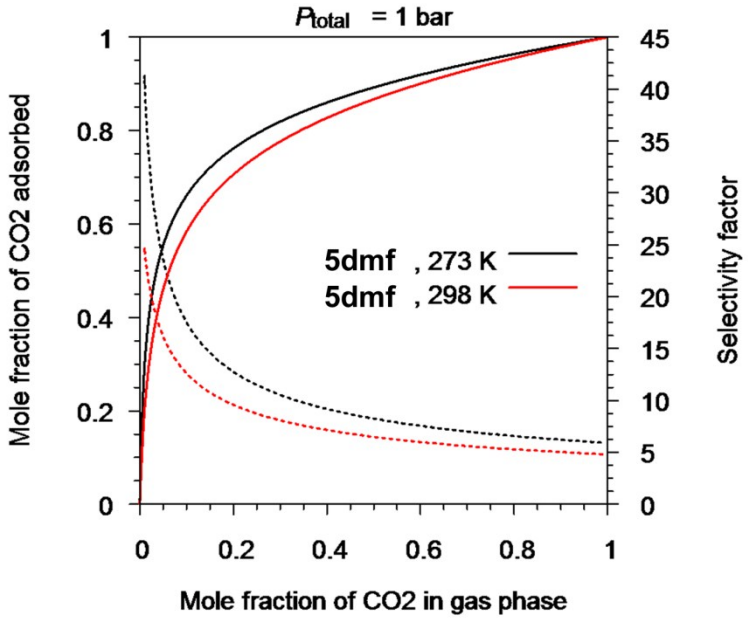

Figure S22. The adsorption equilibrium prediction by IAST for CO_2/CH_4 binary mixture on **5dmf** (solid lines) and the dependence of CO_2/CH_4 adsorption selectivity on the CO_2 mole fraction in gas phase (dashed lines) at 273 K and 298 K.

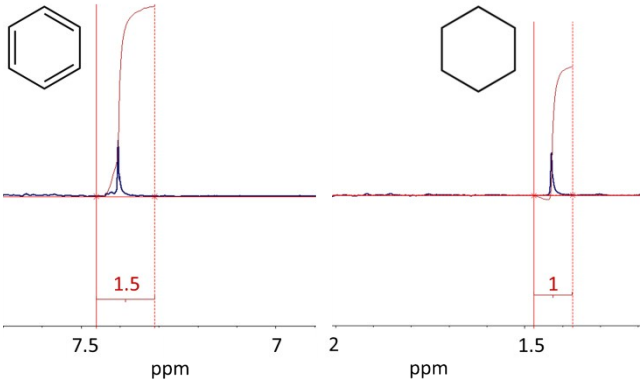

Figure S23. ^{1}H-NMR spectrum of $[LiZn(btb)(dmf)_2(H_2O)_2]$ exposed to a solution of a benzene/cyclohexane mixture (1:1) for 24 hours. Adsorbed benzene and cyclohexane were extracted with DMF:DMF-d^7 solution. The ratio of benzene and cyclohexane in this compound is 3:1.

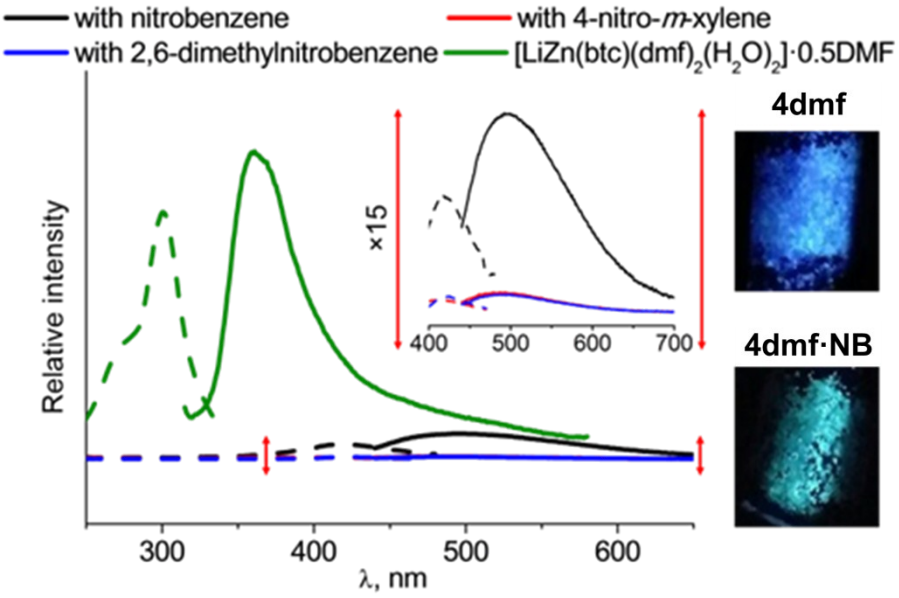

Figure S24. Spectra of emission (solid) and excitation (dashed) of **4dmf** and inclusion compounds (λ_{Ex} = 300 nm, spectral slit width = 3 mm for **4dmf·NB;** 420 nm, 4 mm for guest-exchanged samples). Microfotographs of luminescent species of **4** as synthesized and with nitrobenzene.

REFERENCES:

1. A.L. Myers, J.M. Prausnitz, Thermodynamics of mixed-gas adsorption, AIChE J. 11 (1965) 121–127. doi:10.1002/aic.690110125